Pergamon

Available online at www.sciencedirect.com
SCIENCE DIRECT®

Cement and Concrete Research 33 (2003) 1251–1256

CEMENT AND CONCRETE RESEARCH

Characterization of mercury- and zinc-doped alkali-activated slag matrix Part I. Mercury

Guangren Qian[a,*], Darren Delai Sun[b], Joo Hwa Tay[b]

[a]School of Environment Engineering, Shanghai University, No. 149, Yanchang Road, 200072 Shanghai, PR China
[b]Environmental and Engineering Research Center, School of Civil and Environment Engineering, Nanyang Technological University, Singapore, Singapore

Received 6 June 2002; accepted 31 January 2003

Abstract

The physical properties, pore structure, hydration process and hydration products of mercury-doped (Hg-doped) alkali-activated slag (AAS) matrixes have been evaluated by examination of physical properties, pore structure analysis and XRD, TG-DTG, FTIR and TCLP methods. Low concentrations of Hg^{2+} ions had little effect on the compressive strength, pore structure and degree of hydration of AAS matrixes. The addition of 2% Hg^{2+} ions into the AAS matrix brought out an evident retardation on early hydration and reduction of early compressive strength, but no negative effects were noticed after hydration for 28 days. The results also show that up to 2% of Hg^{2+} ions can be effectively immobilized in the AAS matrix, with the leaching meeting the TCLP mercury limit. Two mechanisms, physical encapsulation and chemical fixation, are assumed to be responsible for the immobilization of mercury in the AAS matrix.

Keywords: Mercury; Immobilization; Alkali-activated slag matrix; Hydration products and physical properties

1. Introduction

Heavy metals, particularly mercury and zinc, are important environmental pollutants that threaten the health of human populations and natural ecosystems alike. Removal of these species from the environment is thus a major focus of waste treatment. Ordinary Portland cement (OPC)/soluble silicate system is one of the matrixes that could effectively solidify and stabilize heavy metals.

The positive roles of soluble silicate in the matrix of OPC/soluble silicate have been reported by many researches [1]. Soluble silicates reduce the leachability of toxic metal ions by the formation of low-solubility amorphous metal silicate precipitates, which are nonstoichiometric compounds coordinated to silanol group SiOH [2]. The chemical and physical bonding by the gel are reported as the mechanisms holding heavy metal ions in the OPC/soluble silicate matrix [3].

Apart from the OPC/soluble silicate system, sodium silicate or water glass has also been used for a long time as an alkali activator to produce alkali-activated slag (AAS) binder [4]. The granulated blast furnace slag in the AAS matrix reacts with soluble sodium silicate to produce poor crystallized C-S-H [5,6]. The C-S-H product appears to have a much bigger immobilization potential for heavy metals [7–9]. Compared to the OPC matrix, the AAS matrix has a high gel pore volume and a significantly low capillary pore fraction. For this reason, the AAS matrix can be expected to be a good material for solidifying heavy metal ions.

The effects of mercury on the hydration and microstructure of the OPC matrix have been studied previously [10–13], but little is known concerning the characterization of mercury-doped (Hg-doped) AAS matrix. In the OPC matrix, physical precipitation was considered as the controlling mechanism for immobilization of mercury, in which the mercury salt tends to hydrolyse to form a red precipitate of HgO in an alkali hydroxide solution or in the environment of cement hydration [10,11]. However, Poon and Perry [12] and Poon et al. [13] established that a combination of the chemical and physical isolation process should be responsible for the containment of mercury.

In this paper, the solidification behaviour of mercury salt in the AAS matrix is reported.

* Corresponding author. Fax: +86-21-56333052.
E-mail address: grqian@mail.shu.edu.cn (G. Qian).

0008-8846/03/$ – see front matter © 2003 Elsevier Science Ltd. All rights reserved.
doi:10.1016/S0008-8846(03)00045-0

2. Experiments

2.1. Materials and immobilization matrixes

The blast furnace slag used for AAS matrix was from Malaysia Steel and Iron Corporation. The chemical composition of this slag is 40.31% CaO, 34.47% SiO_2, 9.47% Al_2O_3, 0.53% Fe_2O_3 and 7.81% MgO. This slag had a specific surface area of 480m^2 /kg. All the pastes of the solidification matrix were prepared with a sodium silicate solution/slag ratio of 0.3. The SiO_2/Na_2O of alkali solution was kept at 2.0 by the addition of NaOH. Four dosages of Hg^{2+} ions at 0%, 0.1%, 0.5% and 2.0% by mass of the slag were added with $HgNO_3{\cdot}H_2O$ into the sodium silicate solution and then moulded into cubes ($50 \times 50 \times 50$ mm). All specimens were cured at room temperature at 100% relative humidity for 1, 3, 7, 14 and 28 days.

2.2. Examination of physical properties

The setting time of the paste was detected according to ASTM C191-2001. After the specimens were cured for certain periods, the compressive strength was also measured according to ASTM C109-2001.

2.3. Leaching test

The TCLP test was conducted according to the EPA-1311 method to evaluate the leaching behaviour of Hg^{2+} ions in the AAS matrixes. The coarse particles after strength test were separated through a 9.5-mm sieve. Fifty grams of particle sample were weighed into a 1000-ml polypropylene plastic bottle, and 1000 ml of the extracting dilute acetic acid (pH = 2.85) solution was added. The suspension was shaken for 18 h in an end-over-end shaker at a speed of 30 rpm. The suspension was then filtered using filter paper. The Hg^{2+} ion concentrations in the filtered solution were measured by the FIMS mercury analysis system.

2.4. Characterization of hydration products

After the strength test, the specimens were crushed into coarse particles or powder and treated with an acetone–alcohol solution to stop the hydration. XRD, TG and FTIR were used to identify the hydration products. The pore size distributions of the matrixes were determined by Micromeritics Autopore III.

3. Results and discussion

3.1. Physical properties

The effects of mercury nitrate on the physical properties of the AAS matrix could be well characterized by the compressive strength and setting time. The AAS paste usually has a quicker setting. As shown in Fig. 1, pure AAS paste with sodium silicate activator (controlled sample) started initial setting within 35 min and reached final setting at 54 min. When mercury nitrate was doped, the setting of AAS paste was retarded. The changes in setting times highly depended on Hg^{2+} ion concentrations. The setting of the paste with 0.1% Hg^{2+} was similar to that of the controlled sample. In the presence of 0.5% Hg^{2+}, the initial and final setting times were 50 and 82 min, respectively. For the 2% Hg^{2+}, the initial setting was prolonged to 80 min and final setting was 170 min, similar to the setting properties of OPC paste.

The compressive strength was also found sensitive to Hg^{2+} ion concentrations. As seen in Fig. 2, the controlled sample had a compressive strength of 55.1 MPa at 3 days. As Hg^{2+} ions were added, the compressive strength at 3 days dropped with the increase of Hg^{2+} ion concentration. Compared to the controlled sample, the samples with 0.1% and 0.5% Hg^{2+} had 10–15% loss of strength at 3 days. For the 2% Hg-AAS matrix, a much worse strength, only 2.5 MPa at 3 days, was detected. With the increase of curing time, however, the compressive strengths of Hg-doped AAS matrix were quickly developed. The strength of the 2% Hg-AAS matrix was enhanced to 49.7 MPa at 7 days. At 28 days, all the Hg-doped AAS matrixes had excellent compressive strength, 70–75 MPa. This suggests that the compressive strength development of Hg-doped AAS pastes at later periods was not affected by Hg^{2+} additions.

3.2. Pore size distribution

The total porosity and pore size distribution is an important indicator of the mechanical properties and leaching potential of the solidification matrix. The pore size distributions of Hg-doped AAS matrixes are illustrated in Fig. 3. The pore structures of Hg-doped AAS matrixes varied with the curing time. From 3 to 7 days, 2% Hg-AAS matrix had a large drop of total porosity and a significant shift towards finer pore size distribution, and subsequently, no significant shift but pore refinement was noticed. It was also noticed that AAS matrixes cured for 28

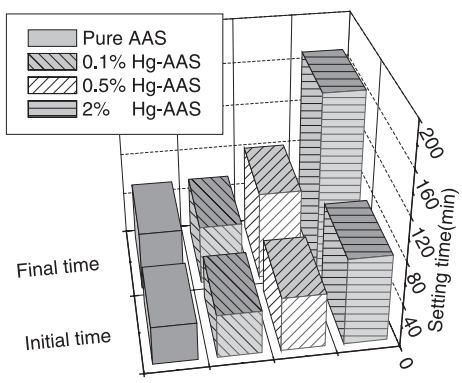

Fig. 1. Setting times of Hg-doped AAS matrixes.

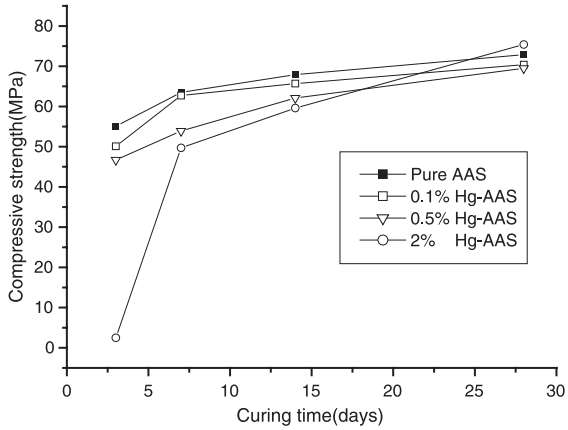

Fig. 2. Compressive strengths of Hg-doped AAS matrixes with curing time.

days, whether or not mercury was added, have almost the same total pore volume (0.10 cm^3/g dry paste), and this volume is less than the corresponding volume of the OPC matrix.

Goto and Roy [14] and Metha [15] suggested that pores larger than 50 to 100 nm may be detrimental to strength and permeability. The pores less than 50 nm in size are somewhat equivalent to the mesopore defined by the International Union of Pure and Applied Chemistry (IUPAC) classification [16]. Fig. 4 illustrates quantitatively the pore size distribution of Hg-doped AAS matrixes. The 2% Hg-AAS matrix possessed a coarser pore size distribution at 3 days, which consisted of 56% micropore (>50 nm) and 44% mesopore. It coincided with its bigger total pore volume at an early period. From 3 to 7 days, the volume of mesopore for this matrix was rapidly increased to 70%, and after that, only minor pore refinement was developed. When cured for 28 days, the 2% Hg-AAS matrix accounted for 75% of mesopore in volume. This mesopore volume was nearly the same as that in the AAS matrixes with 0% and 0.5% mercury at 28 days. This result explains that the pore refinement of the AAS matrix, at the later period of

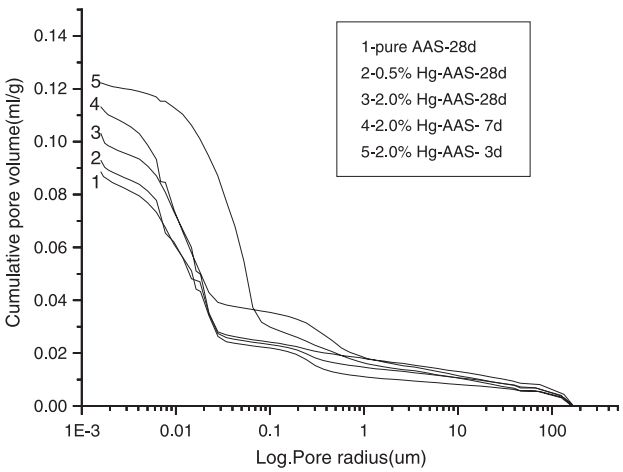

Fig. 3. Cumulative pore size distribution of Hg-doped AAS matrixes.

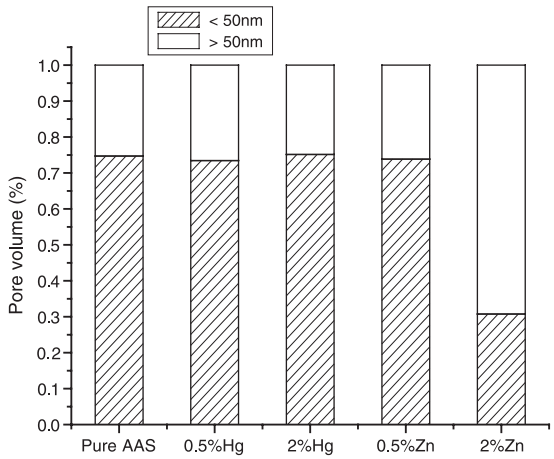

Fig. 4. Mesopore and micropore distribution of Hg-doped matrixes.

hydration, was also not affected by mercury addition, and the mesopore predominated over the pore structure of Hg-doped AAS matrixes.

3.3. Leaching test

Mercury nitrate added in the AAS matrixes was unstable in an aqueous environment, in which it tends to hydrolyse to form a red precipitate of mercury oxide. By observing the colour of samples cured for different ages, it was found that all the 2% Hg-AAS matrixes appeared slightly red in colour. Apparently, this red precipitate should be attributed to the formation of HgO. For the AAS matrixes with 0.1% and 0.5% Hg^{2+}, however, only ordinary grey-black colour occurred.

Fig. 5 shows the leaching results of Hg-doped AAS matrixes detected by TCLP tests. There is a considerable amount of Hg^{2+} leached from 1 to 3 days for all the Hg-doped AAS matrixes. These results were well above the 200 μg/l level, the maximum Hg^{2+} level given in the TCLP guidelines. After being cured for 7 days, the Hg^{2+} amount leached from 0.1% and 0.5% Hg-AAS matrixes decreased

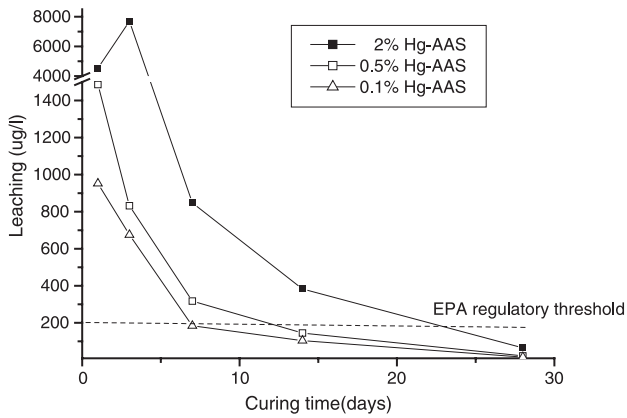

Fig. 5. Leaching of Hg ions from Hg-doped AAS matrixes as a function of curing time by TCLP tests.

to about 200 μg/l. However, the 2% Hg-AAS matrix still had 820 μg/l of Hg^{2+} leaching at 7 days. It was not until 28 days that 2% Hg^{2+} ions could be effectively contained by the AAS matrix to meet the TCLP mercury limit.

Because of the precipitation of less soluble HgO in the 2% Hg-AAS matrix, the rapid drop of Hg^{2+} ions leached from this matrix with time may be related with the formation of HgO in the aqueous environment. However, other matrixes with less than 0.5% Hg^{2+} additions had no trace of precipitation of less soluble HgO, and resulting leaching was still much less. It indicates that another mechanism could be responsible for Hg^{2+} immobilization apart from physical encapsulation of the HgO precipitation.

3.4. Hydration products

Physical properties and microstructures of Hg-doped AAS matrixes are controlled by its hydration process and reaction products, which could be well characterized by XRD, TG-DTG and FTIR methods.

3.4.1. XRD

The XRD results of pure AAS and 2% Hg-AAS matrixes after alkali activation for 28 days are shown in Fig. 6. There is no apparent difference of reaction products between these two samples. No Hg-bearing phases were found. All the samples exhibited a broad and diffuse hump around 29–31° 2θ, which is due to the glass structure of the original slag. A few new peaks superimposed on the amorphous hump at 3.03 and 1.81 Å can be attributed to the formation of poor crystalline C-S-H [5].

Amorphous mercury silicate is supposed to be another reaction product. Iler [17] reported that polyvalent metal salts are easy to react with soluble silicates to produce insoluble amorphous metal silicate precipitates formed by adsorption on gelatinous silica. These reaction products are noncrystalline and gelatinous, and therefore very difficult to be characterized by XRD. The aqueous solution in the sodium silicate–NaOH–slag system keeps a higher pH at around 11. When mercury nitrate was added into the above aqueous solution, a golden gelatinous precipitate was formed. This precipitate was identified as amorphous mercury silicate by DTG and DSC, which would be reported in detail later.

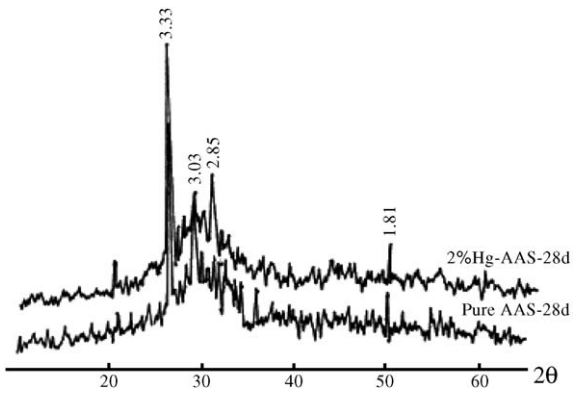

Fig. 6. XRD patterns of Hg-doped AAS matrixes cured for 28 days.

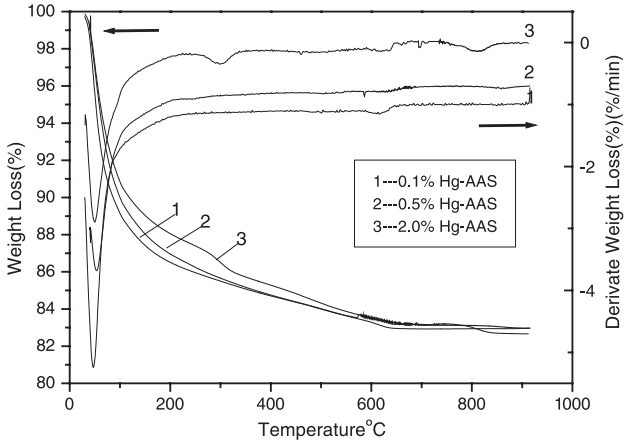

Fig. 7. TG-DTG curves of Hg-doped AAS matrixes cured for 28 days.

3.4.2. TG-DTG

Fig. 7 gives the TG-DTG curves of Hg-doped AAS matrixes cured for 28 days. For all samples, there existed a bigger weight loss with the DTG peak centered at 130 °C, which corresponds to the gradual dehydration of the C-S-H interlayer waster. In addition, only the 2% Hg-AAS matrix showed a steep weight loss between 250 and 350 °C, with the DTG peak centered at 303 °C. Ortego et al. [10] attributed this additional weight loss to the decomposition of HgO into volatile elemental mercury and oxygen. It proves that a new phase HgO was formed in the 2% Hg-AAS matrix and turned the matrix slightly red, whereas this did not occur in the samples with less than 0.5% Hg^{2+}.

The existence of the amorphous mercury silicate precipitate in the Hg-AAS matrix could be detected by TG-DTG. Maliavski et al. [18] found that metal orthosilicate gel had an apparent weight loss due to thermal decomposition in the temperature range of 300–580 °C. As shown in Fig. 8, the

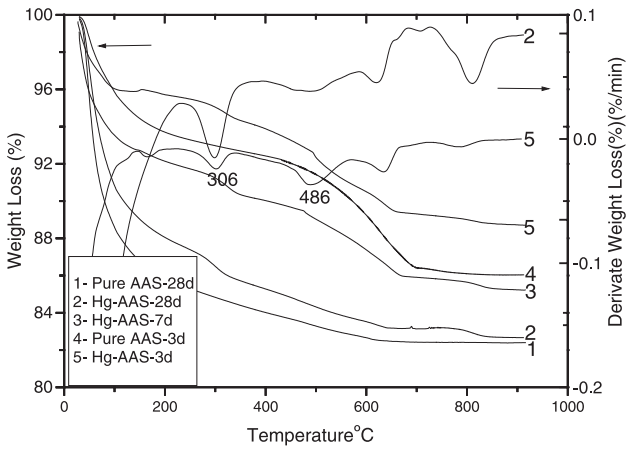

Fig. 8. TG-DTG curves of 2% Hg-doped AAS matrixes cured for different ages.

2% Hg-AAS matrix cured for 3 days had a deep trough of derivate weight loss around 486 °C, and this peak became smoother when cured for 28 days. Judged by Maliavski's results, therefore, this peak around 486 °C should result from the decomposition of amorphous mercury silicate precipitate. The amounts of this precipitate formed in the AAS matrix depended on the dosages of Hg^{2+} ion additions and hydration time. Compared to the 2% Hg-AAS matrix, two other matrixes with 0.1% and 0.5% Hg^{2+} ions had less apparent weight loss around 486 °C at 3 days. This suggests that the addition of Hg favours the formation of an amorphous gelatin phase.

The effects of Hg^{2+} ions on the hydration of AAS matrixes can also be detected by the TG method. As seen in Figs. 7 and 8, the weight loss in all the samples gave nearly a constant value at about 700 °C, indicating that chemically combined water in the AAS matrixes was fully lost. Thus, the magnitude of weight loss at 700 °C in TG curves can be used as an approximate estimation of chemically combined water, which could be related with the degree of hydration in the Hg-doped AAS matrixes at certain periods.

In Fig. 7, the AAS matrixes with 0.1%, 0.5% and 2% had nearly the same weight loss, indicating that they have the same hydration degree at 28 days. Although the 2% Hg-AAS matrix has a much lower hydration degree than pure AAS matrix at 3 days, as seen in Fig. 8, these two matrixes had an almost approximate degree of hydration at 28 days. These results were in accord with other data such as compressive strengths and pore structures, and proved that the effects of Hg^{2+} ions on the hydration process of the AAS matrix depended on the dosages and the periods of hydration. Addition of 2% Hg^{2+} had a significant retardation on early hydration of the Hg-doped AAS matrix, but little effect was noticed after 28 days regardless of Hg^{2+} ion concentration. Whether Hg^{2+} ions have a positive role on latter hydration of AAS matrix is worth exploring.

3.4.3. FTIR

The FTIR results also confirm the existence of C-S-H as a main hydration product. As can be seen in Fig. 9, two

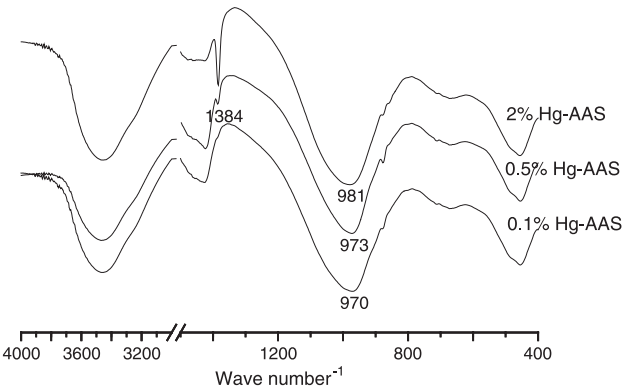

Fig. 9. IR spectra of Hg-doped AAS matrixes cured for 28 days.

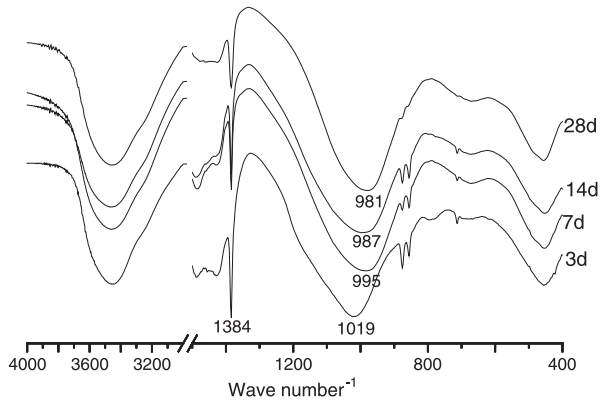

Fig. 10. IR spectra of 2% Hg-doped AAS matrixes cured for different ages.

absorption bands at 3470–3450 and 1655–1650 cm^{-1} appeared in all the samples, which are respectively due to stretching and deformation vibrations of OH and H-O-H groups from water molecules of C-S-H. Another strong absorption band at around 1000 cm^{-1} is attributed to v_3 vibration of Si-O-Si asymmetric stretch mode. As amorphous mercury silicate precipitate is another reaction product containing Si-O-Si stretch bond besides C-S-H [18], this absorption band at around 1000 cm^{-1} should include the contributions from both products. Fig. 9 shows that the v_3 band frequencies of Hg-doped AAS matrixes at 28 days were related with the amount of mercury addition. It shifted from 970 cm^{-1} (0.1% Hg^{2+}) toward higher wave numbers to 973 cm^{-1} (0.5% Hg^{2+}) and 981 cm^{-1} (2% Hg^{2+}) with the increase of Hg^{2+} ion concentration. Previous results [19,20] established that the v_3 band of Si-O-Si is sensitive to the vibration of linkages between the Si-O-Si tetrahedra and the surrounding secondary building blocks of the structure. It indicates that mercury does modify the crystal structure of C-S-H. Mercury ions might be incorporated into the C-S-H and combined into an amorphous mercury silicate precipitate rather than just physically encapsulated.

Furthermore, the v_3 band frequency for 2% Hg-AAS matrix was enhanced with the hydration time. Fig. 10 shows that it shifted toward lower wave numbers from 1019 cm^{-1} at 3 days to 995, 987 and 981 cm^{-1} at 7, 14 and 28 days, respectively. This shift was caused by two factors: (1) silicate ionic groups gradually polymerised during the alkali activation process of slag [21], and (2) more Hg^{2+} ions were gradually combined into reaction products with the progress of hydration time.

3.5. Discussion

Based on the above results, two mechanisms can be predicted for the immobilization of Hg^{2+} ions in the AAS matrix, namely, physical encapsulation and chemical fixation. The contribution of physical encapsulation comes from the refined pore structure of the AAS matrix and the filling of

amorphous metal silicate precipitates in the pore structure, which prevents the less soluble HgO that formed in aqueous environment from physical leaching. The mechanism of chemical fixation is due to the formation of reaction products C-S-H and amorphous metal silicate precipitates. A possible explanation is that Hg^{2+} preferentially reacted with soluble silicate to form insoluble amorphous metal silicate precipitates, then is competitively and gradually bound into the crystal lattice of C-S-H, replacing Ca^{2+} as mercury salt is added into the AAS paste. After that, free Hg^{2+} in the aqueous solution may be reacted to form less soluble HgO as physical encapsulation. This explanation was supported by two facts. Firstly, the forming time of poor crystallized Hg-C-S-H is later than that of amorphous metal silicate precipitates by TG and physical test results. Secondly, the 0.5% Hg-AAS matrix did not have any precipitation of HgO so that only the chemical fixation mechanism could be responsible for the immobilization of mercury in this matrix. However, the relative abilities of these two processes to immobilize mercury in the AAS matrix are still not clear and so more detailed proofs should be collected.

4. Conclusion

Low concentrations of Hg^{2+} ion had little effect on the compressive strength, pore structure and hydration degree of AAS matrixes. Addition of 2% Hg^{2+} into the AAS matrix brought out a significant retardation of early hydration and reduction of early compressive strength, but no negative effects were noticed after hydration for 28 days.

Up to 2% Hg^{2+} can be effectively immobilized in the AAS matrix and the leaching values from these matrixes at 28 days were all lower than the TCLP Hg^{2+} leaching limit.

References

[1] J.R. Conner, Chemical Fixation and Solidification of Hazardous Wastes, Van Nostrand Reinhold, New York, 1990.
[2] J.G. Vail, Soluble Silicates, Reinhold, New York, 1952.
[3] M.E. Tittlebaum, R.K. Seals, F.K. Cartledge, S. Engels, State of the art on stabilization of hazardous organic liquid wastes and sludges, CRC Crit. Rev. Environ. Control 15 (1985) 179–211.
[4] D.M. Roy, Alkali-activated cements opportunities and challenges, Cem. Concr. Res. 29 (1999) 249–254.
[5] S.D. Wang, K.L. Scrivener, Hydration products of alkali activated slag cement, Cem. Concr. Res. 25 (1995) 561.
[6] V.D. Glukhovsky, Soil Silicates, Gosstroi Publishers, Kiev, Ukraine, 1959.
[7] S. Komarneni, E. Breval, D.M. Roy, R. Roy, Reaction of some calcium silicates with metal cations, Cem. Concr. Res. 8 (1978) 204–220.
[8] F.P. Glasser, Material science of cement intended for waste disposal, in: T. White, J.A. Stegemann (Eds.), Environmental Preferred Materials, Advances in Environmental Materials, vol. II, Materials Research Society, Singapore, 2001, pp. 281–291.
[9] F.P. Glasser, Chemistry of cement-solidified waste forms, in: R.D. Spence (Ed.), Chemistry and Microstructure of Solidified Waste Forms, Lewis Publishers, Florida, 1993, pp. 1–38.
[10] J.D. Ortego, S. Jackson, G.S. Yu, H. McWhinney, D.L. Coke, Solidification of hazardous substances—a TGA and FTIR study of Portland cement containing metal nitrates, J. Environ. Sci. Health A24 (1989) 589–602.
[11] H.G. McWhinney, D.L. Cocke, K. Balke, J.D. Ortego, An investigation of mercury solidification and stabilization in Portland cement using X-ray photoelectron spectroscopy and energy dispersive spectroscopy, Cem. Concr. Res. 20 (1990) 79–91.
[12] C.S. Poon, R. Perry, Study of zinc, cadmium and mercury stabilization in OPC/PFA mixtures, in: G.J. McCarthy, F.P. Glasser, D.M. Roy, S. Diamond (Eds.), Materials Research Society Symposium Proceedings: Fly Ash and Coal Conversion By-products Characterization, Utilization and Disposal III, vol. 86, Materials Research Society, Pittsburgh, Pa, 1987, pp. 67–77.
[13] C.S. Poon, A.I. Clark, R. Perry, Permeability study of the cement based solidification process for the disposal, Cem. Concr. Res. 16 (1986) 161–172.
[14] S. Goto, D. Roy, Diffusion of ions through hardened cement pastes, Cem. Concr. Res. 11 (1981) 75–757.
[15] P.K. Metha, Concrete: Its Structure, Properties and Materials, Prentice-Hall, Englewood Cliffs, NJ, 1986.
[16] IUPAC, Manual of symbols and terminology: Appendix 2, Part 1. Colloid and surface chemistry, J. Pure Appl. Chem. 31 (1978) 578.
[17] R.K. Iler, The Chemistry of Silica, Wiley, New York, 1979.
[18] N.I. Maliavski, O.V. Dushkin, G. Scarinci, Low temperature synthesis of some orthosilicates, Ceram.-Silik. 45 (2001) 48–54.
[19] J.S. van Jaarsveld, J.S.J. van Deventer, The effect of metal contaminant of the formation and properties of waste-based geopolymers, Cem. Concr. Res. 29 (1999) 1189–1200.
[20] J.D. Ortego, Y. Barroeta, Leaching effects on silicate polymerisation, an FTIR and ^{29}Si NMR study of lead and zinc in Portland cement, Environ. Sci. Technol. 25 (1991) 1171–1174.
[21] D.L. Cocke, M.Y.A. Mollah, The chemistry and leaching mechanisms of hazardous substances in cementitious solidification/stabilization systems, in: R.D. Spence (Ed.), Chemistry and Microstructure of Solidified Waste Forms, Lewis Publishers, Florida, 1993, pp. 187–242.